Organozinc Complexes with Monoanionic Chelating Phenolates or 2-Pyridylmethanolates. Molecular Structure of [Zn(CH₂SiMe₃){OCH₂(2-Py)}]₄

Paul A. van der Schaaf,[†] Elmo Wissing,[†] Jaap Boersma,[†] Wilberth J. J. Smeets,[‡] Anthony L. Spek,[‡] and Gerard van Koten*,[†]

Department of Metal-Mediated Synthesis, Debye Institute, Utrecht University, Padualaan 8, 3584 CH Utrecht, The Netherlands, and Laboratory of Crystal and Structural Chemistry, Bijvoet Center for Biomolecular Research, Utrecht University, Padualaan 8, 3584 CH Utrecht, The Netherlands

The influence of the chelate ring size and of the presence of sterically demanding groups in the chelating ligand on the degree of association of organozinc *ortho*-substituted phenolates and α-substituted 2-pyridylmethanolates has been studied. Organozinc derivatives were made of phenols with one or two potentially *ortho*-chelating (dimethylamino)methyl groups and of the α-substituted 2-pyridylmethanols, 2-(2-pyridyl)propan-2-ol, 2,4-dimethyl-3-(2-pyridyl)pentan-3-ol, diphenyl-2-pyridylmethanol, 1-phenyl-1-(2-pyridyl)ethanol, and 2,2-dimethyl-1-(2-pyridyl)-propanol. The CH₂NMe₂-substituted phenolate compound 1a, containing a six-membered chelate ring *via* Zn–N coordination is dimeric, whereas compounds 2b and 2b′, having two CH₂NMe₂ substituents in the phenolate ligand, exist in benzene as a monomer–dimer equilibrium. The alkylzinc 2-pyridylmethanolate complexes 3c and 3c′, in which intramolecular Zn–N coordination leads to a five-membered chelate ring, are trimeric in solution. Surprisingly, 3c is a tetramer in the solid state. Introduction of substituents in the five-membered chelate ring of these 2-pyridylmethanolates affects the stability of the aggregates in solution. Complexes 3d and 3g, with small substituents on the α-carbon atoms of the pyridylcarbinolate fragment, exist in solution as equilibria of dimers and trimers, whereas compounds 3e, 3f, and 3h, with more sterically demanding α-substituents, are concentration independent dimers in solution. The molecular structure of tetrameric 3c in the solid state contains a puckered eight-membered Zn₄O₄ ring in which the zinc atoms are coordinatively saturated by four intramolecularly coordinating pyridyl fragments. Crystals of [Zn(CH₂SiMe₃){OCH₂(2-Py)}]₄, 3c, are monoclinic, space group $P2_1/c$ with unit-cell dimensions $a = 12.625(1)$ Å, $b = 17.815(1)$ Å, $c = 12.299(1)$ Å, $\beta = 111.23(1)°$, and final $R = 0.028$.

Introduction

The coordination chemistry of organozinc alkoxides and aryloxides is very diverse.[1–8] Although normally tetrameric association is observed with a distorted cubic Zn₄O₄ core as a common feature,[4,5] the degree of association decreases with increasing bulk of the alkyl and alkoxide groups, resulting in trimeric or dimeric species, *e.g.* [Zn(*t*-Bu)(O-*t*-Bu)]₃[6] and [Zn(CH₂SiMe₃)(OC₆H₂-*t*-Bu₃-2,4,6)]₂.[9] The structure of these complexes also depends on the presence of potentially intramolecular coordinating donor atoms in either the organic or the alkoxide group. Such donor atoms are often involved in intramolecular coor-

dination and may give rise to a very complex coordination behavior.[10]

We have studied a number of alkylzinc complexes derived from phenoxide ligands (a and b), containing one or two potentially coordinating NMe₂ groups, as well as of α-substituted 2-pyridylmethoxides (c–h), in which the size of the α-substituent has been varied (see Figure 1). These organozinc complexes were used as model com-

---

(1) Boersma, J. In *Comprehensive Organometallic Chemistry*; Wilkinson, G., Abel, E., Stone, F. G. A., Eds.; Pergamon: Oxford, U.K., 1984; Vol. 2, Chapter 16.
(2) Coates, G. E.; Ridley, D. *J. Chem. Soc.* 1965, 1870.
(3) Coates, G. E.; Ridley, D. *J. Chem. Soc. A* 1966, 1064.
(4) Shearer, H. M. M.; Spencer, C. B. *J. Chem. Soc., Chem. Commun.* 1966, 194.
(5) Shearer, H. M. M.; Spencer, C. B. *Acta Crystallogr., Sect. B* 1980, B36, 2046.
(6) Noltes, J. G.; Boersma, J. *J. Organomet. Chem.* 1968, 12, 425.
(7) Boersma, J.; Spek, A. L. *J. Organomet. Chem.* 1974, 81, 7.
(8) Boersma, J.; Noltes, J. G. *J. Organomet. Chem.* 1968, 13, 291.
(9) Olmstead, M. M.; Power, P. P.; Shoner, S. C. *J. Am. Chem. Soc.* 1991, 113, 3379.

(10) This enolate is a precursor in the enantioselective organozinc-mediated β-lactam synthesis, see: van der Steen, F. H.; Boersma, J.; Spek, A. L.; van Koten, G. *Organometallics* 1991, 10, 2467.
(11) Knotter, D. M.; Janssen, M. D.; Grove, D. M.; Smeets, W. J. J.; Horn, E.; Spek, A. L.; van Koten, G. *Inorg. Chem.* 1991, 30, 4361.
(12) Haaland, A. *Angew. Chem.* 1989, 101, 1017.
(13) The twice bidentate bonding mode (Figure 6a) has been observed in trimeric [Li{OC₆H₂(CH₂NMe₂)₂-2,6-Me-4}]₃,[14,15] tetrameric [Na{OC₆H₂(CH₂NMe₂)₂-2,6-Me-4}]₄,[15] and two metal phenolate complexes in which one molecule of metal halide is captured, *i.e.* [Li₂I{OC₆H₂(CH₂NMe₂)₂-2,6-Me-4}]₂[14] and [[Cu₂(μ-Br){μ-OC₆H₃(CH₂NMe₂)₂-2,6}][P-(OMe)₃]₂]].[16] The singly bidentate bonding mode (Figure 6b) is present in the high-valent tungsten phenylimido complex [WCl₃(=NPh){OC₆H₄(CH₂NMe₂)₂-2,6-Me-4}][17] and in the aluminum phenolate [Al{OC₆H₂(CH₂NMe₂)₂-2,6-Me-4}₃].[18] In the latter complex two "pincer-phenolate" ligands are single bidentate bonded to aluminum, and the third ligand exhibits a bonding mode shown in Figure 6c, *i.e.* monodentate involving none of the o-CH₂NMe₂ substituents.
(14) van der Schaaf, P. A.; Hogerheide, M. P.; Spek, A. L.; van Koten, G. *J. Chem. Soc., Chem. Commun.* 1992, 1703.
(15) van der Schaaf, P. A.; Jastrzebski, J. T. B. H.; Hogerheide, M. P.; Smeets, W. J. J.; Spek, A. L.; Boersma, J.; van Koten, G. *Inorg. Chem.*, in press.
(16) Wehman, E.; van Koten, G.; Knotter, D. M.; Erkamp, C. J. M.; Mali, A. N. S.; Stam, C. H. *Recl. Trav. Chim. Pays-Bas* 1987, 106, 370.
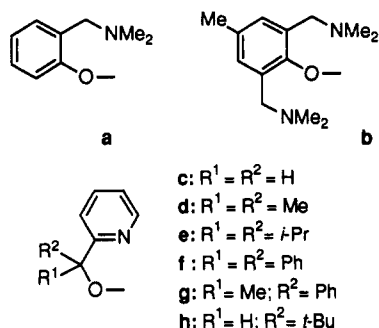

Figure 1. Selected phenolate and alkoxide ligands containing a potentially coordinating amine donor atom.

pounds for a study of the steric and electronic effects of such ligands which, *inter alia*, have been used to prepare some thermally very stable tungsten alkylidene complexes.[17]

Results

The alkylzinc complexes 1–3 were obtained quantitatively by mixing equimolar amounts of bis[(trimethylsilyl)methyl]zinc, dimethylzinc, or dineopentylzinc with the appropriate alcohol in hexane; see Scheme I.

All products are colorless, air and moisture sensitive solids, which were purified by crystallization. Their association behavior in benzene was determined by means of cryoscopy (see Experimental Section, Table I).

[Zn(CH₂SiMe₃)(OC₆H₄CH₂NMe₂-2)], 1a, with one potentially coordinating o-CH₂NMe₂ substituent, is a concentration independent dimer in benzene, whereas [Zn(CH₂SiMe₃){OC₆H₂(CH₂NMe₂)₂-2,6-Me-4}], 2b, with two o-CH₂NMe₂ substituents, is present as a monomer–dimer equilibrium. Replacement of the large (trimethylsilyl)methyl group by a methyl group, as in complex 2b′, did not influence the monomer–dimer ratio in this equilibrium.

The alkylzinc 2-pyridylmethoxides, [Zn(CH₂SiMe₃){OR¹R²(2-Py)}], 3c–3h, are trimers, dimers, or dimer–trimer mixtures depending on the size of the α-substituents (R¹ and R²) in the 2-pyridylmethoxide fragment.

The [(trimethylsilyl)methyl]- and neopentylzinc derivatives of the unsubstituted 2-pyridylmethoxide (R¹ = R² = H), 3c and 3c′, are concentration independent trimers in benzene. The introduction of small substituents on the α-carbon of the 2-pyridylmethoxide fragment, R¹ = R² = Me in 3d and R¹ = Me; R² = Ph in 3g, led to partial dissociation. The compounds containing more sterically demanding substituents on the α-carbon of the 2-pyridylmethoxide fragment (R¹ = R² = i-Pr, 3e; R¹ = R² = Ph, 3f; R¹ = H, R² = t-Bu, 3h) are completely dissociated into dimers. The role of intramolecular coordination in the formation of these aggregates was studied by variable temperature NMR.

The ¹H NMR spectrum of 1a at ambient temperature contains an AB pattern for the benzylic protons and two distinct signals for the NMe₂ methyl groups of the 2-[(dimethylamino)methyl]phenolate moiety, indicating that Zn–N coordination is present and is inert on the NMR time scale. The methylene protons of the CH₂SiMe₃ group also give rise to an AB pattern, indicating the presence of

(17) van der Schaaf, P. A.; Smeets, W. J. J.; Spek, A. L.; van Koten, G. *Inorg. Chem.*, in press.
(18) Hogerheide, M. P.; Wesseling, M.; Spek, A. L.; van Koten, G. To be published.

an inversion center as the only symmetry element in the associate. Therefore, we propose a dimeric structure for 1a, containing a Zn₂O₂ unit with intramolecular coordinating (dimethylamino)methyl groups; see Figure 2. This structure is closely related to that of the recently reported dimeric methylzinc arenethiolate [ZnMe{SC₆H₄CH(Me)-NMe₂-2}]₂, in which the sulfur atoms likewise bridge between two zinc atoms and in which intramolecular Zn–N coordination results in tetrahedrally coordinated zinc atoms.[11]

The resonances of the (dimethylamino)methyl groups and of the alkyl groups in the ¹H and ¹³C NMR spectra of the [(trimethylsilyl)methyl]zinc and methylzinc o-bis-[(dimethylamino)methyl]phenolate complexes, 2b and 2b′, are broad signals both at ambient temperature and at –60 °C. Obviously, fluxional processes and/or intermolecular exchange processes occur that cannot easily be frozen out on the NMR time scale. The observed low apparent molecular weights indicate the presence of a dimer–monomer equilibrium (see Figure 2). The implied monomeric species is not unreasonable since the zinc may attain four-coordination by using both CH₂NMe₂ groups available. The structure of the dimeric species will contain one free o-CH₂NMe₂ group in analogy with the structure proposed for dimeric 1a. Alternating coordination of these o-CH₂NMe₂ substituents to zinc will result in a number of stereoisomers with different chemical shift patterns.

The NMR spectra of the [(trimethylsilyl)methyl]zinc 2-pyridylmethoxides 3d and 3g are not well resolved at ambient temperatures, and even at elevated temperatures (70–80 °C) broad resonances are present. Lowering the temperature to –50 °C gives rise to very complex spectra, especially for 3g, which could not be interpreted unambiguously. In contrast, well-resolved spectra were obtained for the [(trimethylsilyl)methyl]zinc 2-pyridylmethoxides 3e, 3f, and 3h. Complex 3h contains a ligand with a chiral α-carbon atom (R = H; R′ = t-Bu). Consequently, when 3h forms aggregates with a degree of association of 2 or more, mixtures of diastereoisomers can be expected and were indeed found (as a result of bad resolution this was not observed for 3g). It appeared that the ratio of diastereoisomers in 3h is approximately 12:1 (de = 85%).

The NMR spectra of 3e, 3f, and 3h are closely related to those of 1a; *i.e.* they all contain an AB pattern for the methylene hydrogens of the alkyl group, be it at low temperatures for 3e and 3f, indicating that Zn–N coordination is present.

The structures in solution of trimeric [(trimethylsilyl)methyl]- and neopentylzinc 2-pyridylmethoxide 3c and 3c′ were studied by variable temperature NMR spectroscopy. The ¹H NMR spectrum of 3c at ambient temperature shows broad resonances for each of the methylene protons of the (trimethylsilyl)methyl group as well as of the 2-pyridylmethoxide group. At –60 °C, each of these signals splits into three distinct AB patterns; see Figure 3 (only the methylene hydrogens of the 2-pyridylmethoxide ligand are shown). The inequivalence of these methylene groups in the slow exchange limit is also reflected in the ¹³C NMR spectra of 3c and 3c′. At ambient temperature the methylene carbons appear as one signal, whereas at –60 °C three different resonances were observed in a ratio of 1:1:1 (see Experimental Section).

On the basis of these data, the cyclic trimeric structure shown in Figure 4 is proposed for both 3c and 3c′. In this

Scheme I

$$R_2Zn + HOR' \xrightarrow[\text{- RH}]{\text{hexane, RT}} RZnOR'$$

1a : OR' = a; R = CH₂SiMe₃
2b : OR' = b; R = CH₂SiMe₃
2b': OR' = b; R = Me
3c : OR' = c; R = CH₂SiMe₃
3c': OR' = c; R = CH₂CMe₃

3d: OR' = d; R = CH₂SiMe₃
3e: OR' = e; R = CH₂SiMe₃
3f : OR' = f ; R = CH₂SiMe₃
3g: OR' = g; R = CH₂SiMe₃
3h: OR' = h; R = CH₂SiMe₃

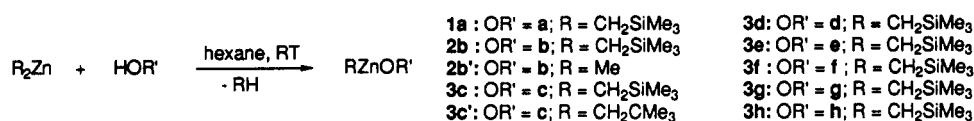**Table I. Results of Cryoscopic Molecular-Weight Determinations of RZnOR' Compounds, 1a–3h[a]**

no.	compd	deg of association
1a	[Zn(CH₂SiMe₃)(OC₆H₄CH₂NMe₂-2)]	1.95
2b	[Zn(CH₂SiMe₃){OC₆H₂(CH₂NMe₂)₂-2,6-Me-4}]	1.50[b]
2b'	[ZnMe{OC₆H₂(CH₂NMe₂)₂-2,6-Me-4}]	1.50[b]
3c	[Zn(CH₂SiMe₃){OCH₂(2-Py)}]	3.00
3c'	[Zn(CH₂CMe₃){OCH₂(2-Py)}]	3.00
3d	[Zn(CH₂SiMe₃){OCMe₂(2-Py)}]	2.20[c]
3e	[Zn(CH₂SiMe₃){OC-*i*-Pr₂(2-Py)}]	2.00
3f	[Zn(CH₂SiMe₃){OCPh₂(2-Py)}]	2.05
3g	[Zn(CH₂SiMe₃){OCMe(Ph)(2-Py)}]	2.15[c]
3h	[Zn(CH₂SiMe₃){OCH(CMe₃)(2-Py)}]	2.00

[a] Measurements were carried out in benzene at two concentrations (see Experimental Section). [b] Indication of monomer–dimer equilibrium. [c] Indication of dimer–trimer equilibrium.
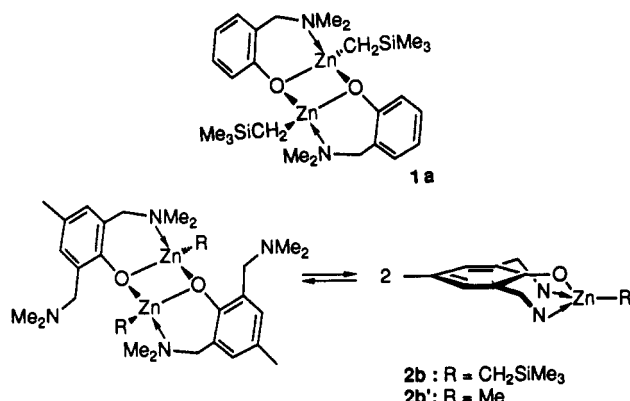

Figure 2. Schematic representation of the dimeric structure of 1a and the dimer–monomer equilibrium of 2b.

25 °C
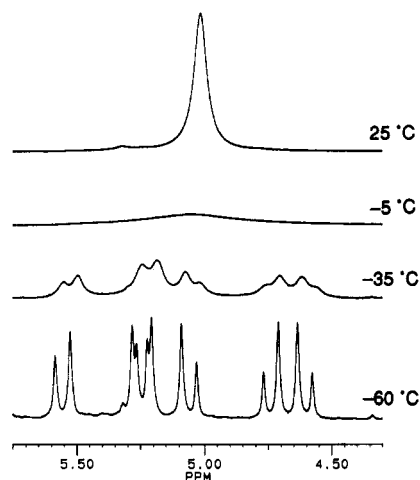
−5 °C

−35 °C

−60 °C

5.50   5.00   4.50
PPM

Figure 3. ¹H NMR spectra of [Zn(CH₂SiMe₃){OCH₂(2-Py)}, 3c, {OC*H₂*(2-Py)} region, in toluene-*d₈* at various temperatures. Three equally large AB patterns are visible at −60 °C.

structure, two 2-pyridylmethoxide ligands lie above and below the Zn₃O₃ plane. This bonding situation gives rise to two enantiomers, differing in the clockwise or anticlockwise sense, in which the chelate rings are closed.

As direct proof for the proposed trimeric structure of 3c, an X-ray structure determination has been carried out. Much to our surprise, in contrast with the trimeric
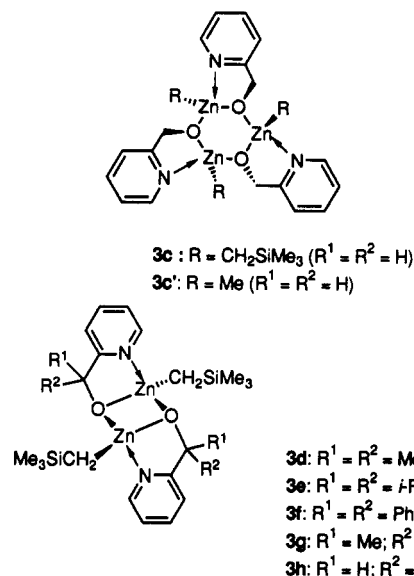

3c : R = CH₂SiMe₃ (R¹ = R² = H)
3c': R = Me (R¹ = R² = H)

3d: R¹ = R² = Me
3e: R¹ = R² = *i*-Pr
3f: R¹ = R² = Ph
3g: R¹ = Me; R² = Ph
3h: R¹ = H; R² = *t*-Bu

Figure 4. Schematic representation of trimeric [Zn(CH₂-SiMe₃){OCH₂(2-Py)}], 3c, and the dimeric structure for 3d–3h.
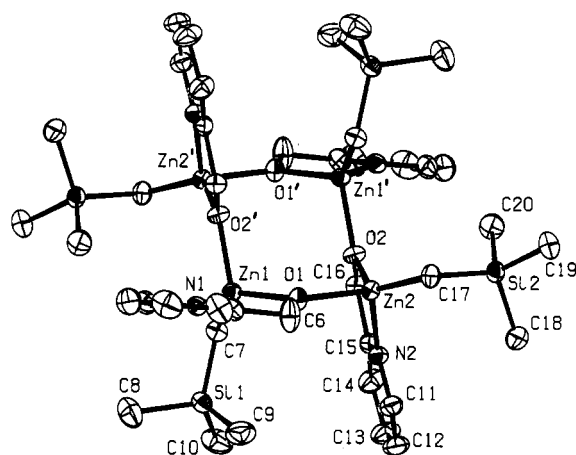

Figure 5. ORTEP drawing (50% probability level) of [Zn-(CH₂SiMe₃){OCH₂(2-Py)}]₄, 3c, with the adopted numbering scheme (H atoms are omitted for clarity).

association found for 3c in a benzene solution, the molecular structure of 3c in the solid state is tetrameric. The crystal structure of 3c involves the packing of two tetramers in a monoclinic unit cell. An ORTEP drawing of 3c along with the adopted numbering scheme is given in Figure 5. Atomic coordinates for 3c as well as selected bond lengths and angles are given in Tables II and III.

The four alkylzinc methoxide units are linked *via* zinc–oxygen–zinc bridges (average Zn–O–Zn angle, 122.58(8)°; average O–Zn–O angle, 101.9(6)°), to give a central, puckered, eight-membered Zn₄O₄ ring. Obviously, intramolecular Zn–N coordination interferes with further coordination by the oxygen atoms. The Zn–O distances in the tetrameric aggregate are nearly identical (ranging from 1.979(2) to 1.987(2) Å; average = 1.985(1) Å). In general, dative Zn–O bonds are significantly longer than Zn–O distances in covalent bonds;[12] *e.g.* in dimeric Zn-

Table II. Fractional Coordinates and Equivalent Isotropic Thermal Parameters for [Zn(CH₂SiMe₃){OCH₂(2-Py)}]₄, 3c

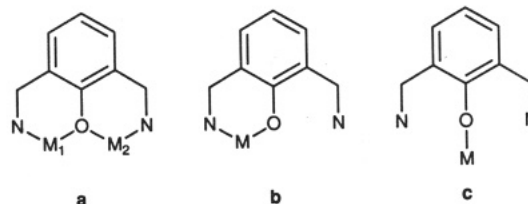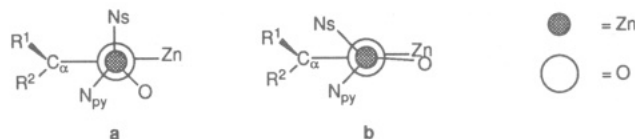| atom	x	y	z	U_{eq},[a] Å^2
Zn(1)	0.82400(2)	0.51199(1)	0.45677(2)	0.0220(1)
Zn(2)	1.03460(2)	0.50096(1)	0.73614(2)	0.0222(1)
Si(1)	0.64460(5)	0.37834(3)	0.43716(5)	0.0276(2)
Si(2)	1.24772(5)	0.50457(3)	0.97793(5)	0.0257(2)
O(1)	0.89787(13)	0.54746(8)	0.62013(12)	0.0261(4)
O(2)	1.08660(13)	0.44096(8)	0.62894(12)	0.0255(5)
N(1)	0.71898(15)	0.60709(10)	0.45205(15)	0.0254(5)
N(2)	0.97426(15)	0.39450(10)	0.76115(15)	0.0247(5)
C(1)	0.6389(2)	0.63875(14)	0.3599(2)	0.0352(7)
C(2)	0.5938(2)	0.70879(15)	0.3643(3)	0.0456(9)
C(3)	0.6327(2)	0.74767(14)	0.4684(3)	0.0497(9)
C(4)	0.7141(2)	0.71521(14)	0.5632(3)	0.0441(9)
C(5)	0.75544(19)	0.64431(12)	0.5527(2)	0.0296(7)
C(6)	0.8424(2)	0.60478(15)	0.6536(2)	0.0440(8)
C(7)	0.77158(19)	0.40814(11)	0.40906(19)	0.0275(6)
C(8)	0.5132(2)	0.40758(17)	0.3156(3)	0.0515(10)
C(9)	0.6399(2)	0.42061(17)	0.5745(2)	0.0497(10)
C(10)	0.6388(2)	0.27381(13)	0.4514(3)	0.0504(10)
C(11)	0.9188(2)	0.37646(13)	0.83250(19)	0.0324(7)
C(12)	0.8853(2)	0.30424(15)	0.8432(2)	0.0417(8)
C(13)	0.9080(2)	0.24887(14)	0.7766(2)	0.0457(9)
C(14)	0.9635(2)	0.26704(13)	0.7016(2)	0.0367(8)
C(15)	0.99701(18)	0.34060(11)	0.69737(18)	0.0244(6)
C(16)	1.06490(19)	0.36398(11)	0.62363(19)	0.0266(6)
C(17)	1.12756(19)	0.55819(11)	0.87696(18)	0.0277(6)
C(18)	1.1971(2)	0.42765(14)	1.0506(2)	0.0397(8)
C(19)	1.3502(2)	0.56465(14)	1.0940(2)	0.0395(8)
C(20)	1.3304(2)	0.45949(14)	0.8963(2)	0.0407(8)

[a] U_{eq} = one-third of the trace of the orthogonalized U.

Table III. Selected Geometrical Data for [Zn(CH₂SiMe₃){OCH₂(2-Py)}]₄, 3c

Bond Lengths (Å)			
Zn(1)–O(1)	1.9872(14)	Zn(2)–O(2)	1.9846(15)
Zn(1)–O(2')	1.9872(16)	Zn(2)–O(1)	1.9795(16)
Zn(1)–N(1)	2.1392(19)	Zn(2)–N(2)	2.1076(18)
Zn(1)–C(7)	1.981(2)	Zn(2)–C(17)	1.986(2)
O(1)–C(6)	1.383(3)	O(2)–C(16)	1.395(2)

Bond Angles (deg)			
O(1)–Zn(1)–O(2')	104.68(6)	Zn(1)–O(1)–Zn(2)	124.28(8)
O(1)–Zn(2)–O(2)	99.12(6)	Zn(2)–O(2)–Zn(1')	120.88(7)
O(1)–Zn(1)–N(1)	80.50(7)	O(2)–Zn(2)–N(2)	80.57(7)
O(1)–Zn(1)–C(7)	125.50(8)	O(2)–Zn(2)–C(17)	128.51(9)
Zn(1)–C(7)–Si(1)	115.79(12)	Zn(2)–C(17)–Si(2)	113.84(10)

(OC₆H₂-*t*-Bu₃)₂(THF)₂ the Zn–O(THF) bonds are 0.2 Å longer than the Zn–O(aryl) bonds.[13]

Figure 6. Bonding modes of the "pincer-phenolate" ligand [–OC₆H₂(CH₂NMe₂)₂-2,6-Me-4].

Figure 7. Two Newman projections along the Zn–O axis in [Zn(CH₂SiMe₃){OCR¹R²(2-Py)}]₃, (a) without and (b) with a "quasi-aromatic" Zn₃O₃ central ring (Ns = CH₂SiMe₃; N$_{py}$ = pyridine nitrogen atom).

Discussion

We have previously reported[8] the first alkylzinc phenolates in which a potentially coordinating nitrogen atom is present, *i.e.* dimeric ethyl- and phenylzinc *N*-phenylsalicylaldiminate. In the case of dimeric [ZnMe{SC₆H₄-CH(Me)NMe₂-2}]₂, **4**,[11] we showed that intramolecular coordination gives rise to a lowering of the degree of association. As expected, complex **1a**, containing one *ortho*-chelating phenolate ligand which is very related to the thiolate ligand in **4**, is also dimeric. When a second potentially *ortho*-chelating substituent is introduced, like in **2b** and **2b'**, a further decrease in associating leads to dimeric aggregates in equilibrium with monomeric species. This decrease may be the result of steric crowding around the zinc and/or of active involvement of both the *o*-CH₂NMe₂ substituents in coordination to the same metal center to satisfy four-coordination at zinc. However, a singly tridentate bonding mode of the "pincer-phenolate" ligand to the ZnR unit as depicted in Figure 2 would involve the formation of two fused six-membered chelate rings,

resulting in a considerably strained molecule. A dimeric aggregate would contain two bidentate bonded pincer-phenolate ligands, *i.e* each having one free *o*-CH₂NMe₂ substituent, together causing steric crowding close to the central Zn₂O₂ core. These destabilizing factors are probably responsible for the observed monomer–dimer equilibrium.

The pincer-phenolate ligand used in these compounds is very flexible and can adapt easily to a number of metal-coordination environments (see Figure 6).[13]

The ligand may be doubly bidentate bonded while the oxygen serves as a bridge between two metal centers (Figure 6a),[14–16] singly bidentate bonded as proposed for dimeric **2b** and **2b'** (Figure 6b),[17,18] or monodentate bonded using only the phenolate oxygen (Figure 6c).[18] In this light, the possibility that it may act as a single tridentate ligand, as we postulated for the monomeric form of **2b** and **2b'**, is not unlikely.

All complexes described so far are dimers or dimer-monomer equilibria and contain potentially chelating groups in positions that result in the formation of six-membered chelate rings upon intramolecular coordination. When the potential chelate ring size is decreased from six- to five-membered, trimeric aggregation is observed, as in **3c** and **3c'**. Ethylzinc complexes containing quinolin-8-olate and 2-(dimethylamino)ethoxide as the chelating ligand, both capable of forming a five-membered chelate ring, were earlier found to be trimeric in solution.[8] The introduction of bulky substituents in a potential five-membered chelate ring leads to further dissociation, and dimer formation becomes favorable. Thus, the trimeric aggregation in **3c** and **3c'** changes into dimeric association in **3e–3h** upon the introduction of sterically demanding groups. The central Zn₃O₃ ring in a trimeric aggregate is assumed to be "quasi-aromatic";[14,15,19,20] *i.e.* the Zn₃O₃ ring is nearly planar through electron donation by the oxygen atoms. The planarity of this ring implies that the alkyl group at zinc is forced into the proximity of the substituent on the α-carbon atom of the chelating ligand; see Figure 7. In the presence of large substituents, steric interference will disfavor trimeric association in favor of a dimeric association. Steric interactions are assumed to play a leading role also in the diastereoselective formation of

(19) Power, P. P. *J. Organomet. Chem.* **1990**, *400*, 49.
(20) Olmstead, M. M.; Power, P. P.; Shoner, S. C. *J. Am. Chem. Soc.* **1991**, *113*, 3379.

complex **3h**, containing a chiral α-carbon atom in the chelate ring substituted with a *tert*-butyl group.

Although **3c** is a trimer in benzene solution, its molecular structure in the solid state is a tetramer. The latter is closely related to the solid state structure of an ethylzinc enolate resulting from the deprotonation of Me(*t*-Bu)-NCH$_2$COOMe with (*N,N*-diisopropylamido)ethylzinc,[10] which was the first example of a tetrameric zinc enolate containing an eight-membered Zn$_4$O$_4$ ring. In both compounds the zinc atoms, which are bridged by two alkoxide oxygens, are four-coordinate by intramolecular Zn–N coordination and the bond distances and angles within the Zn$_4$O$_4$ core are very similar.

The observed difference between the degrees of association of **3c** in solution and in the solid state may well arise from preferential crystallization of a tetrameric species which is slightly soluble and is present in small quantities in solutions of **3c**. This equilibrium must lie far to the side of trimeric aggregates, as no evidence for the presence of other aggregates could be detected in solutions of **3c** using either cryoscopy or NMR spectroscopy.

The coordination behavior in solution of the alkylzinc alcoholates and phenolates described here is based on the strong electrophilic character of the zinc in these compounds. Intermolecular coordination of the zinc to alcoholate and phenolate oxygens gives rise to the formation of trimeric or tetrameric associates. Intramolecular coordination of the zinc to electronegative atoms present in the groups bound to zinc via oxygen generally lowers the degree of association and dimers or dimer–monomer equilibria are observed. It was found that the size of the chelate rings formed during intramolecular association and the size of the substituents present in these rings finally determine the degree of association.

Experimental Section

General Information. All reactions were performed in an atmosphere of dry, deoxygenated nitrogen, using standard Schlenk techniques. All solvents were dried and distilled under nitrogen prior to use. 2-Pyridylcarbinol is commercially available and was distilled prior to use. ZnMe$_2$,[21] Zn(CH$_2$SiMe$_3$)$_2$,[22] 2-[(dimethylamino)methyl]phenol,[23] 2-(2-pyridyl)propan-2-ol,[24] 1-phenyl(2-pyridyl)ethanol,[25] and diphenyl-2-pyridylmethanol[26] were prepared by standard literature methods. 2,6-Bis[(dimethylamino)methyl]-4-methylphenol and 2,4-dimethyl-3-(2-pyridyl)pentan-3-ol were synthesized *via* procedures similar to those described in the literature for 2-[(dimethylamino)methyl]-phenol and diphenyl-2-pyridylmethanol, respectively. Room temperature ^{1}H and ^{13}C NMR spectra were recorded on a Bruker AC 200 or AC 300 spectrometer in benzene-d_6. Variable temperature ^{1}H and ^{13}C NMR spectra were recorded on the same spectrometers with toluene-d_8 as solvent. The cryoscopic measurements presented in Table I were performed in benzene (the accuracy of these measurements is estimated to be about 5%). Elemental analyses were carried out at the Institute for Applied

Chemistry TNO, Zeist, The Netherlands, or at the Mikroanalytisches Laboratorium Dornis und Kolbe, Mülheim a.d. Ruhr, Germany.

General Synthetic Procedure. Equimolar amounts of ROH and dialkylzinc compound were mixed in pentane or hexane at room temperature and stirred for at least 4 h (reactions with the phenols are complete within 1 h). Evaporation of the volatiles yields the desired alkylzinc complex in nearly quantitative yield. The products were purified by crystallization from hexane or toluene. The synthesis of **3e** was carried out in diethyl ether, and the product was crystallized from the same solvent.

Analytical Data. [Zn(CH$_2$SiMe$_3$)(OC$_6$H$_3$CH$_2$NMe$_2$-2)] (1a). ^{1}H NMR (25 °C): δ 7.26–6.73 (m, 4, Ar–H), 4.38 (d, 1, $^2J_{H_AH_B}$ = 12.2 Hz, CH_AH$_B$N), 2.61 (d, 1, $^2J_{H_BH_A}$ = 12.2 Hz, CH$_A$$H_B$N), 2.36 (s, 3, NMe), 1.72 (s, 3, NMe), 0.06 (s, 9, SiMe$_3$), –1.02 (d, 1, $^2J_{H_AH_B}$ = 12.5 Hz, CH_AH$_B$Si), –1.09 (d, 1, $^2J_{H_BH_A}$ = 12.5 Hz, CH$_A$$H_B$Si). ^{13}C NMR (25 °C), δ: 162.9 (C$_{ipso}$), 131.4, 130.6, 125.5, 120.9, 118.5 (Ar C); 63.1 (CH$_2$N); 46.5, 44.8 (NMe); 3.2 (SiMe$_3$); –12.3 (CH$_2$Si). ^{1}H NMR (100 °C): δ 7.12–6.63 (m, 4, Ar–H), 3.4 (br s, 2, CH$_2$N), 2.15 (br s, 6, NMe$_2$), –0.09 (s, 9, SiMe$_3$), –1.16 (s, 2, CH$_2$Si). Anal. Calcd for C$_{13}$H$_{23}$NOSiZn: C, 51.57; H, 7.66; N, 4.63. Found: C, 51.35; H, 7.41; N, 4.58. Molecular weight determined by cryoscopy (conc (wt %): 0.78, 1.44): calcd for monomer 302.9; found 568, 608.

[Zn(CH$_2$SiMe$_3$){OC$_6$H$_2$(CH$_2$NMe$_2$)$_2$-2,6-Me-4}] (2b). ^{1}H NMR (25 °C): δ (*m*-H, not observed; CH$_2$N, not observed), 2.23 (s, 3, *p*-Me), 2.2 (br, 12, N*Me$_2$*), 0.07 (s, 9, SiMe$_3$), –1.06 (s, 2, CH$_2$Si). ^{13}C NMR (25 °C), δ: 158.1 (C$_{ipso}$); 130.8, 128.3–127.0 (Ar C); 61 (br, CH$_2$N); 46.1 (br, NMe$_2$); 20.8 (*p*-Me); 3.5 (SiMe$_3$); –11.9 (CH$_2$Si). ^{1}H NMR (100 °C): δ 6.98 (s, 2, *m*-H), 3.64 (s, 4, CH$_2$N), 2.21 (s, 12, NMe$_2$), 2.18 (s, 3, *p*-Me), –0.09 (s, 9, SiMe$_3$), –1.15 (s, 2, CH$_2$Si). ^{1}H NMR (–30 °C), δ: 7.71, 6.56 (2s, s, *m*-H); 4.57 (d, 1, $^2J_{H_AH_B}$ = 11.8 Hz, CH_AH$_B$N-coord); 3.81 (d, 1, $^2J_{H_AH_B}$ = 14.2 Hz, CH_AH$_B$N-free); 3.68 (d, 1, $^2J_{H_BH_A}$ = 14.2 Hz, CH$_A$$H_B$N-free); 2.59 (d, 1, $^2J_{H_BH_A}$ = 11.8 Hz, CH$_A$$H_B$N-coord); 2.37 (s, 6, NMe$_2$-free); 2.35 (s, 3, NMe-coord); 2.26 (s, 3, *p*-Me); 1.58 (s, 3, NMe-coord); 0.14 (s, 9, SiMe$_3$); –1.04 (d, 1, $^2J_{H_AH_B}$ = 12.3 Hz, CH_AH$_B$Si); –1.17 (d, 1, $^2J_{H_BH_A}$ = 12.30 Hz, CH$_A$$H_B$Si). Anal. Calcd for C$_{17}H_{32}N_2$OSiZn: C, 54.61; H, 8.63; N, 7.49. Found: C, 54.21; H, 8.20; N, 7.43. Molecular weight determined by cryoscopy (conc (wt %): 0.61, 1.12): calcd for monomer 373.9; found 556, 591.

[ZnMe{OC$_6$H$_2$(CH$_2$NMe$_2$)$_2$-2,6-Me-4}] (2b′). ^{1}H NMR (25 °C): δ 6.97 (s, 2, *m*-H), 3.65 (br s, 4, CH$_2$N), 2.23 (s, 3, *p*-Me), 2.09 (s, 12, NMe$_2$), –0.56 (ZnMe). ^{13}C NMR (25 °C), δ: 158.8 (CO); 131.3, 127.1, 126.4 (Ar C); 6.13 (CH$_2$N); 45.9 (NMe$_2$); 20.8 (*p*-Me); –18.9 (ZnMe). ^{1}H NMR (–90 °C), δ: 7.81, 6.53 (2s, 2, *m*-H); 4.70 (br s, 1, half AB pattern CH$_2$N-coord); 3.61 (br s, 2, CH$_2$N-free); 2.4 (very br, 13, NMe$_2$-free, NMe-coord, *p*-Me, half AB pattern CH$_2$N-coord); 1.49 (br s, 3, NMe-coord); –0.46 (s, 3, ZnMe). Anal. Calcd for C$_{14}$H$_{24}$N$_2$OZn: C, 55.73; H, 8.02; N, 9.28. Found: C, 55.53; H, 7.84; N, 9.16. Molecular weight determined by cryoscopy (conc (wt %): 0.85, 1.58): calcd for monomer 301.7; found 444, 462.

[Zn(CH$_2$SiMe$_3$){OCH$_2$(2-Py)}] (3c). ^{1}H NMR (25 °C), δ: 8.22, 6.88–6.44 (m, 4, Ar–H); 5.07 (br s, 2, CH$_2$O); 0.14 (s, 9, SiMe$_3$); –0.69 (br s, 2, CH$_2$Si). ^{13}C NMR (25 °C), δ: 164.8, 146.8, 137.6, 122.2, 120.6 (pyridyl C); 67.9 (C$_\alpha$); 3.4 (SiMe$_3$); –10.8 (CH$_2$Si). ^{1}H NMR (60 °C), δ (all signals sharpened): 8.23 (d, 1), 6.97 (t, 1), 6.65–6.53 (m, 2) (pyridyl H); 5.01 (s, 2, CH$_2$O); 0.02 (s, 9, SiMe$_3$); –0.87 (2, CH$_2$Si). ^{1}H NMR (–40 °C), δ (three different pyridyl ligands were observed with three AB patterns for both the CH$_2$O and CH$_2$Si hydrogens): AB patterns CH$_2$O hydrogens 5.57, 5.25 (dd, $^2J_{H,H}$ = 17.6 Hz), 5.25, 5.05 (dd, $^2J_{H,H}$ = 17.7 Hz), 4.76, 4.61 (dd, $^2J_{H,H}$ = 17.5 Hz); AB patterns CH$_2$Si hydrogens 0.08, –0.07 (dd, $^2J_{H,H}$ = 11.9 Hz), –0.37, –0.58 (dd, $^2J_{H,H}$ = 12.4 Hz), –1.02, –1.85 (dd, $^2J_{H,H}$ = 12.2 Hz); SiMe$_3$ signals at 0.49, 0.14, and –0.04. ^{13}C NMR (–60 °C), δ: 68.5, 68.1, 67.4 (CH$_2$O); 4.3, 3.8, 3.3 (SiMe$_3$); –10.0 (2), –12.6 (CH$_2$Si). Anal. Calcd for C$_{10}$H$_{17}$NOSiZn: C, 46.07; H, 6.57; N, 5.37. Found: C, 45.46; H, 6.56; N, 5.16. Molecular weight determined by cryoscopy (conc (wt %): 2.24, 5.65): calcd for monomer 260.7; found 806, 751.

(21) Galyer, A. L.; Wilkinson, G. *Inorg. Synth.* **1979**, *19*, 253.

(22) Zn(CH$_2$SiMe$_3$)$_2$ was prepared from LiCH$_2$SiMe$_3$ and ZnCl$_2$ in diethyl ether. Lit. ref LiCH$_2$SiMe$_3$: Sommer, L. H.; Mitch, F. A.; Goldberg, G. M. *J. Am. Chem. Soc.* **1949**, *71*, 2746.

(23) (a) Décombe, J. *C. R. Seances Acad. Sci.* **1933**, *196*, 866. (b) Bayer & Co. Deutsches Reichspatent No. 89979 and 92309; *Frdl.* **1895**, *4*, 103.

(24) Luz, W. D.; Fallab, S.; Erlenmeyer, H. *Helv. Chim. Acta* **1955**, *38*, 1114.

(25) Davies, A. G.; Kenyon, J.; Thaker, K. *J. Am. Chem. Soc.* **1956**, *78*, 3394.

(26) Wibaut, J. P.; De Jonge, A. P.; Van der Voort, H. P. G.; Otto, P. Ph. H. L. *Rec. Trav. Chim. Pays-Bas* **1951**, *70*, 1054.

[Zn(CH₂CMe₃){OCH₂(2-Py)}] (3c′). ¹H NMR (25 °C), δ: 8.25, 6.6.94, 6.58, 6.50 (d, t, t, d, 4, pyridine H); 5.05 (br s, 2, CH₂O); 1.10 (s, 9, CMe₃); 0.61 (br s, 2, CH₂C). ¹³C NMR (25 °C), δ: 165.2, 146.8, 137.3, 122.1, 120.5 (pyridyl C); 68.1 (C_α); 35.9 (CMe₃); 27.2 (CH₂C). ¹H NMR (−60 °C), δ (three different pyridyl ligands were observed with three AB patterns for both the CH₂O and CH₂C hydrogens): AB patterns CH₂O hydrogens 5.69, 5.33 (dd, ²J_{H,H} = 17.8 Hz), 5.33, 5.16 (dd, ²J_{H,H} = 17.9 Hz), 4.74 (s, ²J_{H,H} = not observed); AB patterns CH₂C hydrogens 1.49, 1.34 (dd, ²J_{H,H} = 12.3 Hz), 1.03, 0.92 (dd, ²J_{H,H} = 12.9 Hz), 0.61, −0.23 (dd, ²J_{H,H} = 12.4 Hz); CMe₃ signals at 1.62, 1.13, and 1.10. ¹³C NMR (−60 °C), δ: 68.9, 68.5, 67.6 (CH₂O); 36.7, 36.2, 36.0 (CMe₃); 27.9 (2), 25.9 (CH₂C). Anal. Calcd for C₁₁H₁₇NOZn: C, 54.01; H, 7.00; N, 5.73. Found: C, 53.76; H, 7.05; N, 5.78. Molecular weight determined by cryoscopy (conc (wt %): 1.57, 5.48): calcd for monomer 244.6; found 746, 714.

[Zn(CH₂SiMe₃){OCMe₂(2-Py)}] (3d). ¹H NMR (25 °C), δ: 8.31, 7.92, 6.87, 6.78, 6.32 (br Ar H); 1.65 (s, 6, CMe₂); 0.20 (br s, 9, SiMe₃); −0.67 (br s, 2, CH₂Si). ¹H NMR (70 °C), δ (all signals sharpened): 7.95 (d, 1), 7.00–6.64 (m, 2), 6.42 (t, 1) (pyridyl H); 1.59 (s, 6, CMe₂); 0.11 (s, 9, SiMe₃); −0.79 (2, CH₂Si). ¹³C NMR (70 °C), δ: 171.3 (CO); 146.4, 137.5, 121.5, 120.3 (Ar C); 75.0 (C_α); 33.8 (CMe₂); 3.4 (SiMe₃); −5.7 (CH₂Si). Anal. Calcd for C₁₂H₂₁NOSiZn: C, 49.91; H, 7.33; N, 4.85. Found: C, 49.84; H, 7.49; N, 4.83. Molecular weight determined by cryoscopy (conc (wt %): 1.77, 4.02): calcd for monomer 294.7; found 678, 634.

[Zn(CH₂SiMe₃){OC-i-Pr₂(2-Py)}] (3e). ¹H NMR (25 °C), δ: 8.17, 6.96, 6.90, 6.56 (d, t, d, t, 4, pyridyl H); 2.29 (dq, 2, CHMe₂); 0.96, 0.80 (2d, 12, CHMe₂). ¹³C NMR (25 °C), δ: 167.4, 146.7, 137.0, 121.9, 121.8 (pyridyl C); 83.9 (C_α); 37.6 (CHMe₂); 19.1, 18.6 (CHMe₂); 4.0 (SiMe₃); −5.5 (CH₂Si). Anal. Calcd for C₁₆H₂₉NOSiZn: C, 55.72; H, 8.48; N, 4.06. Found: C, 55.81; H, 8.42; N, 4.09. Molecular weight determined by cryoscopy (conc (wt %): 1.37, 2.35): calcd for monomer 344.9; found 699, 668.

[Zn(CH₂SiMe₃){OCPh₂(2-Py)}] (3f). ¹H NMR (25 °C), δ: 7.45 (br s, 4), 7.33 (d, 1), 7.16–7.03 (m, 6), 6.97 (d, 1), 6.71 (t, 1), 6.31 (t, 1) (Ar H); 0.26 (s, 9, SiMe₃); −0.76 (s, 2, CH₂Si). ¹³C NMR (25 °C), δ: 166.7, 150.4, 146.4, 136.9, 129.1, 128.0, 127.2, 125.2, 121.7 (Ar C); 85.0 (C_α); 3.7 (SiMe₃); −6.7 (CH₂Si). Anal. Calcd for C₂₂H₂₅NOSiZn: C, 64.00; H, 6.10; N, 3.39. Found: C, 63.87; H, 6.17; N, 3.34. Molecular weight determined by cryoscopy (conc (wt %): 1.95, 3.42): calcd for monomer 412.9; found 846, 867.

[Zn(CH₂SiMe₃){OCMe(Ph)(2-Py)}] (3g). ¹H NMR (25 °C): only broad resonances are observed. ¹H NMR (80 °C), δ: 8.0, 7.4, 7.1, 6.9, 6.5 (br m, 9, Ar H); 2.02 (br s, 3, CMe); −0.01 (br s, 9, SiMe₃); −0.99 (br s, 2, CH₂Si). ¹³C NMR (80 °C), δ (badly resolved): 169, 147, 137.4, 127.5, 123, 121 (Ar C); 79.5 (CMe); 33 (CMe); 3.3 (SiMe₃); −6 (CH₂Si). Anal. Calcd for C₁₇H₂₃NOSiZn: C, 58.20; H, 6.61; N, 3.99. Found: C, 58.26; H, 6.68; N, 4.08. Molecular weight determined by cryoscopy (conc (wt %): 0.64, 2.19): calcd for monomer 350.8; found 758, 744.

[Zn(CH₂SiMe₃){OCH(CMe₃)(2-Py)}] (3h). Two diastereo-isomers are observed in a ratio of approximately 12:1. ¹H NMR (25 °C) (major isomer), δ: 8.30, 6.89, 6.83, 6.43, (d, d, t, t, 4, pyridyl H); 4.92 (s, 1, OCHCMe₃); 0.97 (s, 9, CMe₃); 0.30 (s, 9, SiMe₃); −0.67 (badly resolved AB pattern, 2, CH₂Si). ¹H NMR (25 °C) (minor isomer), δ: 7.75, 6.8, 6.15, 6.08 (d, d, t, t, 4, pyridyl H); 4.20 (s, 1, OCHCMe₃); 0.93 (s, 9, CMe₃); 0.52 (s, 9, SiMe₃); −0.33 (br s, 2, CH₂Si). ¹³C NMR (25 °C) (major isomer), δ: 165.5, 146.9, 136.9, 124.2, 122.5 (pyridyl C); 84.7 (C_α); 37.6 (CMe₃); 27.0 (CMe₃); 3.7 (SiMe₃); −10.2 (CH₂Si). Anal. Calcd for C₁₄H₂₅NOSiZn: C, 53.08; H, 7.95; N, 4.42. Found: C, 53.18; H, 7.88; N, 4.49. Molecular weight determined by cryoscopy (conc (wt %): 0.71, 1.60): calcd for monomer 316.8; found 647, 612.

X-ray Structure Determination of Complex 3c. X-ray data were collected on a CAD-4T rotating anode diffractometer (Mo Kα, graphite monochromated, 150 K) for a transparent colorless plate-shaped crystal. Pertinent data are given in Table IV. A total of 11 028 reflections were scanned and corrected for *Lp*, a small linear decay, and absorption/extinction (DIFABS,²⁷ cor-

Table IV. Crystal Data and Details of the Structure Determination of Complex 3c

Crystal Data	
formula	Zn₄C₄₀H₆₈N₄O₄Si₄
mol wt	1042.91
cryst syst	monoclinic
space group	P2₁/c (No. 14)
a, b, c (Å)	12.625(1), 17.815(1), 12.299(1)
β (deg)	111.23(1)
V (Å³)	2578.6(4)
Z	2
D_calc (g cm⁻³)	1.343
F(000)	1088
μ (cm⁻¹)	20.1
cryst size (mm)	0.20 × 0.40 × 0.62

Data Collection	
temp (K)	150
θ_min, θ_max (deg)	1.14, 27.5
radiation	Mo Kα (graphite), 0.710 73 Å
Δω (deg)	0.60 + 0.35 tan θ
hor and vert aperture (mm)	2.99, 4.0
linear decay (%)	4
ref reflns	1,−5,2, −5,−2,3, 2,−4,−4
data set	−16:16; 0:23; −15:15
total no. of data, no. of unique data, R_int	11 028, 5899, 0.02
no. of obsd data [I > 2.5σ(I)]	4788

Refinement	
no. of refined params	254
no. of reflns	4788
weighting scheme	$1/[\sigma^2(F) + 0.000196F^2]$
final R, R_w, S	0.028, 0.032, 1.07
max and av shift/error[a]	0.33, 0.02
min, max resd dens (e/Å³)	−0.34, 0.38

[a] All refined parameters were within one-third of their esd and were therefore considered completely refined.

rection range 0.84:1.10). The structure was solved with DIRDIF92²⁸ and refined on F by full-matrix least-squares techniques (SHELX-76).²⁹ All hydrogens were introduced at calculated positions and refined riding on their carrier atom (C–H = 0.98 Å) with one common isotropic U parameter. Scattering factors were taken from Cromer and Mann³⁰ and corrected for anomalous dispersion.³¹ Geometric calculations, including the illustrations, were done with PLATON-92³² on a DEC5000/Ultrix system.

Supplementary Material Available: Tables of anisotropic thermal parameters, all H atom parameters, bond lengths, and bond angles (5 pages). Ordering information is given on any current masthead page.

OM930121Q

(27) Walker, N.; Stuart, D. *Acta Crystallogr., Sect. A* **1983**, *39*, 158.

(28) Beurskens, P. T.; Admiraal, G.; Beurskens, G.; Bosman, W. P.; Garcia-Granda, S.; Gould, R. O. The DIRDIF Program System; Technical Report of the Crystallographic Laboratory; University of Nijmegen: The Netherlands, 1992.

(29) Sheldrick, G. M. *SHELX76. Crystal structure analysis package*; University of Cambridge: Cambridge, England, 1976.

(30) Cromer, D. T.; Mann, J. B. *Acta Crystallogr., Sect. A* **1968**, *24*, 321.

(31) Cromer, D. T.; Liberman, D. *J. Chem. Phys.* **1970**, *53*, 1891.

(32) Spek, A. L. *Acta Crystallogr., Sect. A* **1990**, *46*, C34.